Atmospheric
Chemistry
and Physics

Supplement of

Evaluating the impact of new observational constraints on P-S/IVOC emissions, multi-generation oxidation, and chamber wall losses on SOA modeling for Los Angeles, CA

Prettiny K. Ma et al.

Correspondence to: Patrick L. Hayes (patrick.hayes@umontreal.ca)

6 Estimation of SOA yields for the MA model cases by accounting for chamber vapor losses

7   The approach used here to estimate SOA yields for VOC oxidation that account for losses of gas phase organic compounds to the
8   walls of Teflon environmental chambers uses a set of recently published parameters for modeling gas-wall partitioning in chamber
9   experiments (Krechmer et al., 2016). This previous work found that the fraction of each compound that partitioned to the walls at
10 equilibrium followed absorptive partitioning theory with an equivalent wall mass concentration that could be calculated from the
11 following equation.

12
$$c_w = 16(c^*)^{0.6} \; \mu g \; m^{-3} \quad for \; c^* = 1, 10, 100, or \; 1000 \; \mu g \; m^{-3} \qquad (1)$$

13 Our approach assumes equilibrium between the organic material found in the gas phase, particle phase, and the chamber walls. The
14 limitations of this assumption and its potential impact on the model results are discussed below. The partitioning of the SVOCs
15 between the particle and gas phases and the chamber walls can be calculated using the particle concentration, C_{OA} as well as the
16 equivalent wall mass concentration calculated from Equation 1 above.

$$\frac{[SVOC]_w}{[SVOC]_g} = \frac{c_w}{c^*} \qquad (2)$$

$$\frac{[SVOC]_p}{[SVOC]_g} = \frac{c_{OA}}{c^*} \qquad (3)$$

17 Furthermore, the yield, α_i, is the total amount of SVOC at a given volatility, i, formed from a given VOC.

$$[SVOC]_{g,i} + [SVOC]_{p,i} + [SVOC]_{w,i} = \alpha_i \, [\Delta VOC] \qquad (4)$$

18 Combining Equations 2, 3, and 4, one can obtain the following equation.

$$[SVOC]_{p,i} = \alpha_i \left(1 + \frac{C_i^*}{C_{OA}} + \frac{C_{w,i}}{C_{OA}}\right)^{-1} [\Delta VOC] \qquad (5)$$

19 If a four bin basis set is used where i = 1, 10, 100, or 1000 μg m^{-3}, then the total SOA yield, Y, measured during an environmental
20 chamber experiment can be fit with Equation 6, which is simply Equation 5 summed over the four volatilities and then rearranged.

$$Y = \alpha_1 \left(1 + \frac{1}{C_{OA}} + \frac{C_{w,1}}{C_{OA}}\right)^{-1} + \alpha_{10} \left(1 + \frac{10}{C_{OA}} + \frac{C_{w,10}}{C_{OA}}\right)^{-1} + \alpha_{100} \left(1 + \frac{100}{C_{OA}} + \frac{C_{w,100}}{C_{OA}}\right)^{-1}$$

$$+ \alpha_{1000} \left(1 + \frac{1000}{C_{OA}} + \frac{C_{w,100}}{C_{OA}}\right)^{-1} \tag{6}$$

The corrected yields in this work were determined by simulating yield curves using the parameters published in Tsimpidi et al. (2010) and then refitting the curves using Equation 6.

For clarity, c_w is the equivalent organic mass concentration of the walls, and it is an empirically determined value. Equations 2 and 3 are the partitioning equations that describe either the partitioning between the gas phase and walls or the gas phase and the particles, which both depend on the volatility of the organic vapors, c^*. The significance of c_w can be understood by comparing equations 2 and 3. In equation 3, the partitioning is dependent on the total particle phase, c_{OA}. Similarly, the parameter c_w is the amount of mass in the chamber walls available for partitioning expressed as an effective mass concentration based on the work of Krechmer et al. (2016). However, the value of c_w is a function of c^* as shown in equation 1.

As mentioned above, the approach described here assumes equilibrium between the particle and gas phases as well as the chamber walls. For higher volatility compounds ($c^* \geq 10$ µg m^{-3}), this assumption is reasonable given recently published results that show transfer of mass between particles and walls on the timescale of an hour (Ye et al., 2016). The same paper has shown however that for compounds with a volatility of $c^* = 1$ µg m^{-3}, the organic material condensed on particles evaporates and partitions to the chamber walls on timescales that are longer than typical chamber experiments. The α value for the $c^* = 1$ µg m^{-3} bin would then be biased high since the model described above would attribute mass to the chamber walls that is not actually present. Therefore, the amount of V-SOA in model cases that use the corrected yields determined here should be considered an upper limit. Furthermore, the original yields (without aging) should be considered lower limits.

Estimation of the SVOC volatility distribution at Pasadena from Thermonuder Aerosol Mass Spectrometry Measurements (TD-AMS)

The TD-AMS measurements at Pasadena were carried out using the system previously described by Huffman et al. (2008). Briefly, switching valves were used to sample both ambient air as well as ambient air passed through a thermodenuder (TD) that was scanned between 37 and 260°C. The mass fraction remaining (MFR) as a function of temperature, also known as a thermogram, is

42 then calculated from the ratio of the TD measurements and the linearly-interpolated ambient measurements. In order to compare
43 against the model, the thermogram was only determined for the period between 12:00 – 15:00 local time, which corresponded to 5 h of
44 photochemical aging at a reference OH concentration of 1.5×10^6 molec OH cm^{-3}. This thermogram is shown below in Figure S11.
45 The thermogram is then converted to a volatility distribution using the method described by Faulhaber et al. (2009).

46   The lowest volatility bin modeled is $c^* = 0.01$ µg m^{-3}, but similar to previous measurements (Dzepina et al., 2011), the TD
47 volatility distribution extends to lower volatility bins. The mass in these lower bins is lumped into the $c^* = 0.01$ bins to allow
48 comparison with the model. In addition, since the background SOA is treated as non-volatile in the box model, we subtract the amount
49 of background SOA from the lowest bin ($c^* = 0.01$ µg m^{-3}) after lumping to determine the volatility distribution of urban OA at
50 Pasadena. Both of these approximations will bias the measured urban OA towards higher volatilities. When subtracting the
51 background SOA, this bias would be due to the possibility that some of the background SOA is found in c^* bins greater than 0.01 µg
52 m^{-3}. Thus, some of the mass subtracted from the $c^* = 0.01$ µg m^{-3} bin should instead be subtracted from more volatile bins. Given the
53 measured urban OA is already lower volatility than that predicted in the model, correcting these potential sources of error would not
54 change the conclusion in the main text that the measured SOA is less volatile than the modeled SOA.

55

REFERENCES

Dzepina, K. Cappa, C. D. Volkamer, R. M. Madronich, S. DeCarlo, P. F. Zaveri, R. A. and Jimenez, J. L.: Modeling the Multiday Evolution and Aging of Secondary Organic Aerosol During MILAGRO 2006, Environ. Sci. Technol., 45, 3496-3503, 2011

Faulhaber, A. E. Thomas, B. M. Jimenez, J. L. Jayne, J. T. Worsnop, D. R. and Ziemann, P. J.: Characterization of a thermodenuder-particle beam mass spectrometer system for the study of organic aerosol volatility and composition, Atmos. Meas. Tech., 2, 15-31, 2009

Huffman, J. A. Ziemann, P. J. Jayne, J. T. Worsnop, D. R. and Jimenez, J. L.: Development and characterization of a fast-stepping/scanning thermodenuder for chemically-resolved aerosol volatility measurements, Aerosol Sci. Technol., 42, 395-407, 2008

Krechmer, J. E. Pagonis, D. Ziemann, P. J. and Jimenez, J. L.: Quantification of Gas-Wall Partitioning in Teflon Environmental Chambers Using Rapid Bursts of Low-Volatility Oxidized Species Generated in Situ, Environ. Sci. Technol., 50, 5757-5765, 2016

Tsimpidi, A. P. Karydis, V. A. Zavala, M. Lei, W. Molina, L. Ulbrich, I. M. Jimenez, J. L. and Pandis, S. N.: Evaluation of the volatility basis-set approach for the simulation of organic aerosol formation in the Mexico City metropolitan area, Atmos. Chem. Phys., 10, 525-546, 2010

Ye, P. Ding, X. Hakala, J. Hofbauer, V. Robinson, E. S. and Donahue, N. M.: Vapor wall loss of semi-volatile organic compounds in a Teflon chamber, Aerosol Sci. Technol., 50, 822-834, 2016

74 **Table S1.** Parameters for VOC oxidation used in the model. The aging rate constant for the multi-generation oxidation of VOCs is
75 1×10^{-11} cm^3 molec^{-1} s^{-1}.

Classification	Compounds	Molecular weight (g mol^{-1})	k_{OH} (cm^3 molec^{-1} s^{-1})	ΔVOC/ΔCO (ppt ppb^{-1})	Stoichiometric SOA yield High-NOx, 298 K (µg m^{-3})				
					0.1	1	10	100	1000
Alk5	Methylcyclopentane	84.2	5.68×10^{-12}	0.566	0.000	0.000	0.150	0.000	0.000
	Cyclohexane		6.97×10^{-12}	0.285					
	Methylcyclohexane	98.2	9.64×10^{-12}	0.202					
	n-Heptane	100.2	6.76×10^{-12}	0.398					
	2-Methylhexane		6.89×10^{-12}	0.385					
	3-Methylhexane		7.17×10^{-12}	0.460					
	2,3-Dimethylpentane		7.15×10^{-12}	0.252					
	2,4-Dimethylpentane		4.77×10^{-12}	0.171					
	2,2,3-Trimethylbutane		3.81×10^{-12}	0.031					
	n-Octane	114.2	8.11×10^{-12}	0.197					
	3-Methylheptane		8.59×10^{-12}	0.131					
	2-Methylheptane		8.31×10^{-12}	0.171					
	2,2,4-Trimethylpentane		3.34×10^{-12}	0.476					
	2,3,4-Trimethylpentane		6.60×10^{-12}	0.171					
	2,3,3-Trimethylpentane		4.40×10^{-12}	0.194					
	n-Nonane	128.3	9.70×10^{-12}	0.220					
	n-Decane	142.3	1.10×10^{-11}	0.180					
	Undecane	156.3	1.23×10^{-11}	0.290					
Ole1	Propene	42.1	2.63×10^{-11}	3.740	0.000	0.001	0.005	0.038	0.150
	1-Butene	56.1	3.14×10^{-11}	0.340					
	1-Pentene	70.1	3.14×10^{-11}	0.112					
	2-Methyl-1-Butene		6.10×10^{-11}	0.250					
	3-Methyl-1-Butene		3.18×10^{-11}	0.058					
Ole2	1,3-butadiene	54.1	6.66×10^{-11}	0.350	0.000	0.003	0.026	0.083	0.270
	trans-2-pentene	70.1	6.70×10^{-11}	0.097					
	cis-2-pentene		6.50×10^{-11}	0.050					

Table S1 (continued).

Classification	Compounds	Molecular weight (g mol^{-1})	k_{OH} (cm^3 molec^{-1} s^{-1})	ΔVOC/ΔCO (ppt ppb^{-1})	Stoichiometric SOA yield High-NOx, 298 K (μg m^{-3})				
					0.1	1	10	100	1000
Ole2	Styrene	104.2	5.80×10^{-11}	0.220	0.000	0.003	0.026	0.083	0.270
Ald	Benzaldehyde	106.1	1.15×10^{-11}	1.15×10^{-9}	0.000	0.000	0.000	0.000	0.000
	o-Tolualdehyde	120.1							
	m-Tolualdehyde								
	p-Tolualdehyde								
	2,5-Dimethylbenzaldehyde	134.2							
Aro1	Toluene	92.1	5.63×10^{-12}	3.180	0.000	0.003	0.165	0.300	0.435
	Ethylbenzene	106.2	7.00×10^{-12}	0.570					
	i-Propylbenzene	120.2	6.30×10^{-12}	0.030					
	n-Propylbenzene		5.80×10^{-12}	0.110					
	Benzene	78.1	1.22×10^{-12}	1.300					
Aro2	o-Ethyltoluene	120.2	1.19×10^{-11}	0.120	0.000	0.002	0.195	0.300	0.435
	m/p-Ethyltoluene		1.52×10^{-11}	0.349					
	1,2,3-Trimethylbenzene		3.27×10^{-11}	0.240					
	1,2,4-Trimethylbenzene		3.25×10^{-11}	0.620					
	1,3,5-Trimethylbenzene		5.67×10^{-11}	0.310					
	m/p-Xylene	106.2	1.87×10^{-11}	1.790[a]					
	o-Xylene		1.36×10^{-11}	0.459[b]					
Isop	Anthropogenic isoprene	68.1	1.00×10^{-10}	0.300	0.000	0.001	0.023	0.015	0.000
	Biogenic isoprene			N/A					
Terp	α-pinene + β-pinene + limonene	136.2	9.82×10^{-11}	N/A	0.000	0.012	0.122	0.201	0.500

77 [a]Average of both emission ratios; [b]Zhao et al. 2014

78

79 **Table S2.** Parameters for P-IVOC oxidation used in the model. Measurements of the IVOCs were reported in Zhao et al. 2014. The
80 aging rate constant for the multi-generation oxidation of P-IVOCs is 4×10^{-11} cm^3 molec^{-1} s^{-1}.

Classification	Compounds	k_{OH} (cm^3 molec^{-1} s^{-1})	ΔIVOC/ΔCO (ng m^{-3} ppb^{-1})	Stoichiometric SOA yield High-NOx, 298 K (µg m^{-3})				
				0.1	1	10	100	1000
Naph	Naphtalene	2.44×10^{-11}	0.341	0.000	0.165	0.005	0.516	0.881
	1-Methylnaphtalene	4.09×10^{-11}	0.058					
	2-Methylnaphtalene	4.86×10^{-11}	0.110					
	Phenanthrene	3.20×10^{-11}	0.187					
Alk10	B12 alkane	1.32×10^{-11}	1.718	0.000	0.150	0.000	0.000	0.000
Alk11	B13 alkane	1.51×10^{-11}	1.513					
Alk12	Dodecane	1.32×10^{-11}	0.446	0.000	0.014	0.110	0.160	0.000
	B14 alkane	1.68×10^{-11}	0.951					
	B12 cyclic	1.32×10^{-11}	8.950					
Alk13	Tridecane	1.51×10^{-11}	0.310	0.014	0.059	0.220	0.400	0.000
	Heptylcyclohexane	1.91×10^{-11}	0.049					
	B15 alkane	1.82×10^{-11}	0.574					
	B13 cyclic	1.51×10^{-11}	5.868					
Alk14	Tetradecane	1.68×10^{-11}	0.479	0.022	0.094	0.300	0.350	0.000
	Octylcyclohexane	2.05×10^{-11}	0.049					
	B16 alkane	1.96×10^{-11}	0.486					
	B14 cyclic	1.68×10^{-11}	5.009					
Alk15	Pentadecane	1.82×10^{-11}	0.277	0.044	0.071	0.410	0.300	0.000
	Nonylcyclehexane	2.19×10^{-11}	0.036					
	Pristane	2.44×10^{-11}	0.062					
	B17 alkane	2.10×10^{-11}	0.795					
	B15 cyclic	1.82×10^{-11}	2.758					
Alk16	Hexadecane	1.96×10^{-11}	0.204	0.053	0.083	0.460	0.250	0.000
	Decylcyclohexane	2.33×10^{-11}	0.029					
	Phytane	2.61×10^{-11}	0.031					
	B18 alkane	2.24×10^{-11}	0.278					

81   **Table S2 (Continued).**

Classification	Compounds	k_{OH} (cm^3 molec^{-1} s^{-1})	ΔIVOC/ΔCO (ng m^{-3} ppb^{-1})	Stoichiometric SOA yield High-NOx, 298 K (μg m^{-3})				
				0.1	1	10	100	1000
Alk16	B16 cyclic	1.96×10^{-11}	1.855	0.053	0.083	0.460	0.250	0.000
Alk17	Heptadecane	2.10×10^{-11}	0.141	0.063	0.089	0.550	0.200	0.000
	Octadecane	2.24×10^{-11}	0.070					
	Nonadecane	2.38×10^{-11}	0.030					
	Eicosane	2.52×10^{-11}	0.015					
	Heneicosane	2.67×10^{-11}	0.010					
	B19 alkane	2.38×10^{-11}	0.123					
	B20 alkane	2.52×10^{-11}	0.072					
	B21 alkane	2.67×10^{-11}	0.028					
	B17 cyclic	2.10×10^{-11}	2.473					
	B18 cyclic	2.24×10^{-11}	0.939					
	B19 cyclic	2.38×10^{-11}	0.526					
	B20 cyclic	2.52×10^{-11}	0.311					
	B21 cyclic	2.67×10^{-11}	0.142					

82

83 **Table S3.** Parameters for P-SVOC oxidation and the P-SVOC volatility distribution used in the model. The volatility distribution of P-
84 SVOCs reported by Worton et al. (2014) is used for vehicular emissions whereas the volatility distribution of P-SVOCs reported by
85 Robinson et al. (2007) is used for cooking emissions.

c^* ($\mu g\ m^{-3}$)	ΔH_{vap} ($kJ\ mol^{-1}$)	Molecular Weight ($g\ mol^{-1}$)	Fraction of total P-SVOC (%)	
ROB & WOR	ROB & WOR	ROB & WOR	ROB	WOR
10^{-2}	112		6	4
10^{-1}	106		12	6
10^{0}	100	250	18	12
10^{1}	94		28	19
10^{2}	88		36	59
K_{OH} ($cm^3\ molec^{-1}\ s^{-1}$)	4×10^{-11}			
Oxygen mass gain per oxidation generation (%)	7.5			
Volatility decrease per oxidation generation	1 order of magnitude			

86

87   **Table S4.** Updated version of the SOA yields for VOCs accounting for losses of semi-volatile gases to chamber walls.

Classification	Stoichiometric SOA yield, High-NO$_X$, at 298 K (μg m^{-3})			
	1	10	100	1000
Alk5	0.157	0.000	0.000	0.000
Ole1	0.014	0.000	0.098	0.088
Ole2	0.052	0.000	0.183	0.157
Ald	0.000	0.000	0.000	0.000
Aro1	0.276	0.002	0.431	0.202
Aro2	0.310	0.000	0.420	0.209
Isop	0.034	0.000	0.005	0.000
Terp	0.210	0.000	0.348	0.297

88
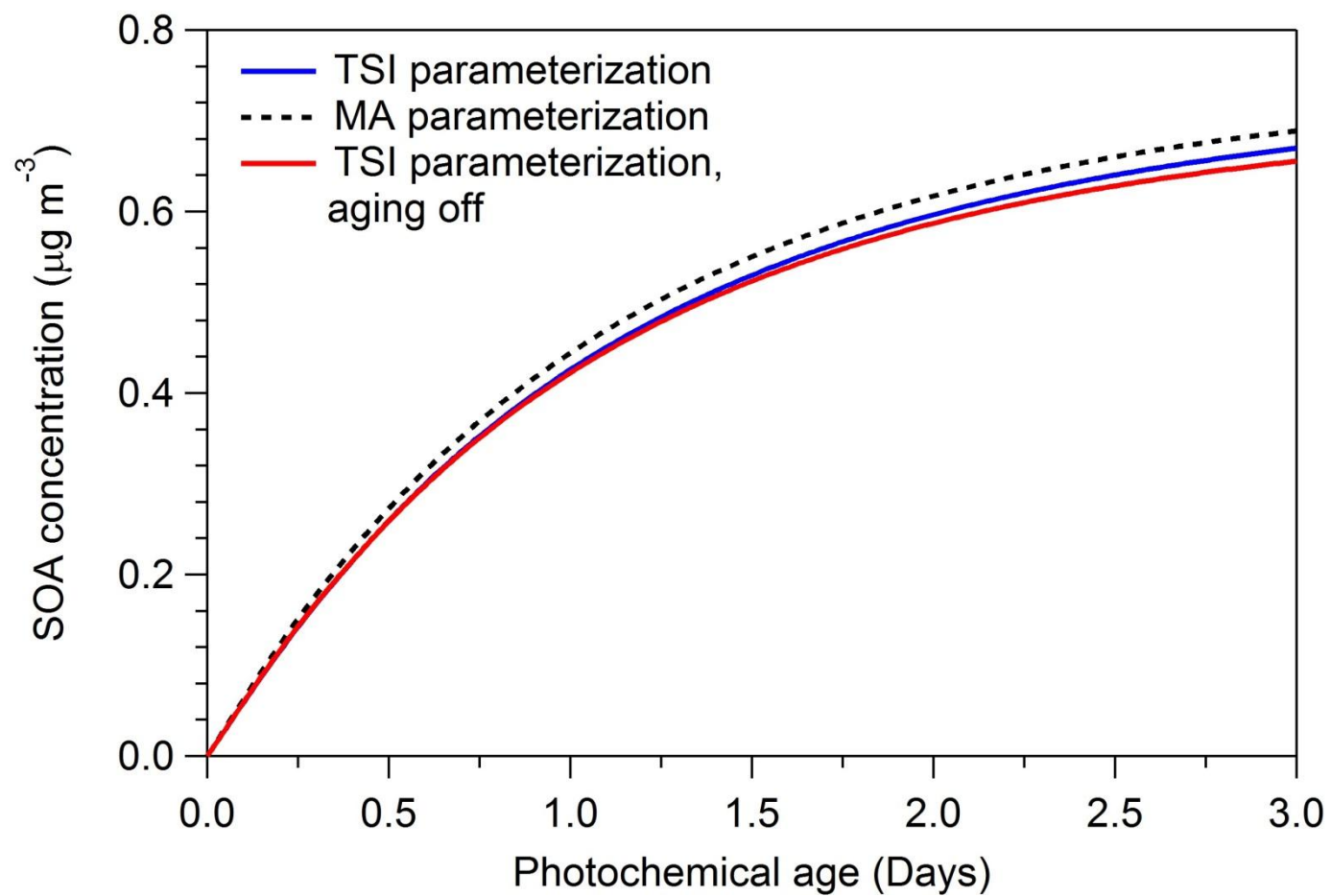
89

90 **Figure S1.** Predicted urban SOA mass from the alkane VOCs (Alk5) for different SOA formation parameterizations.
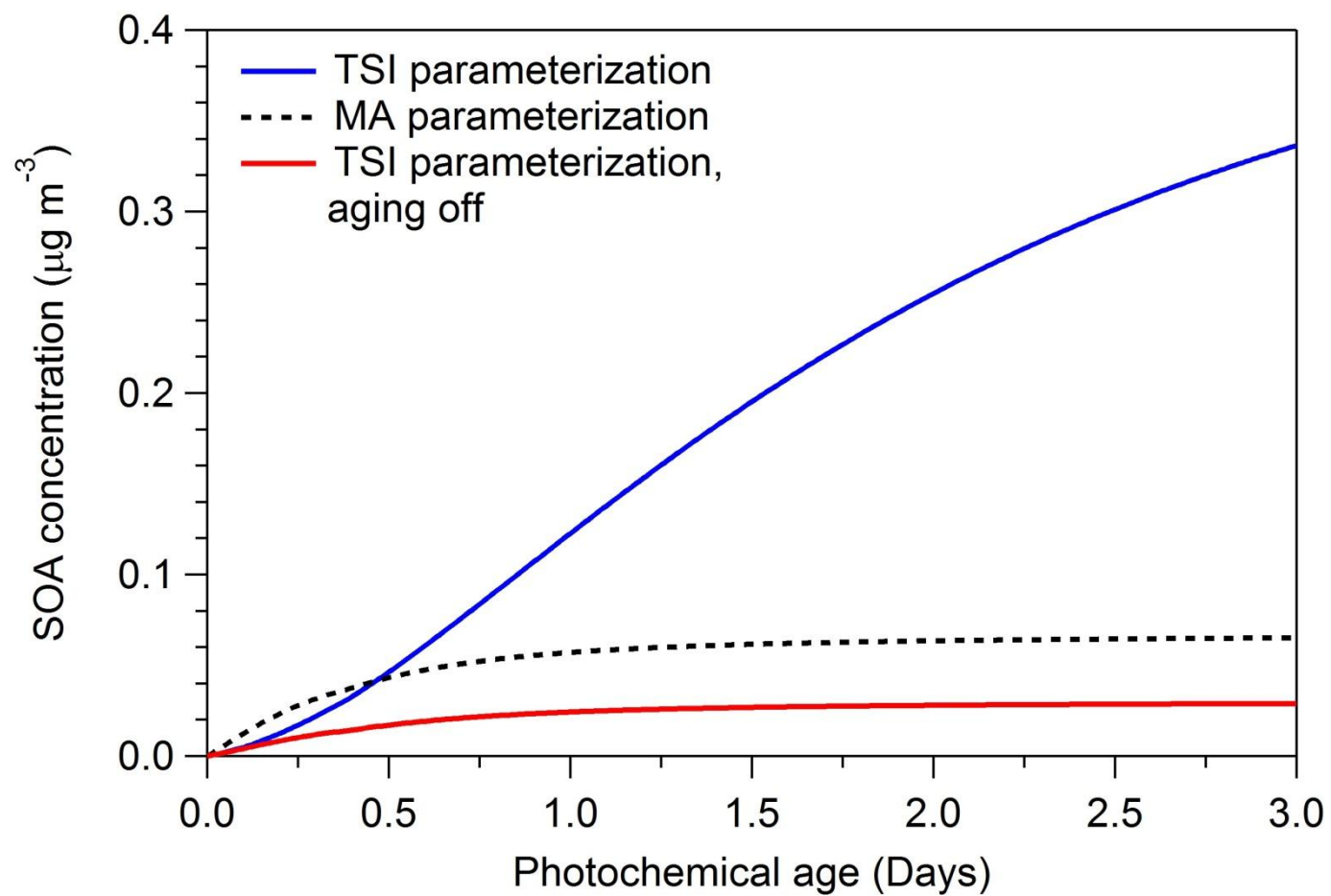
91

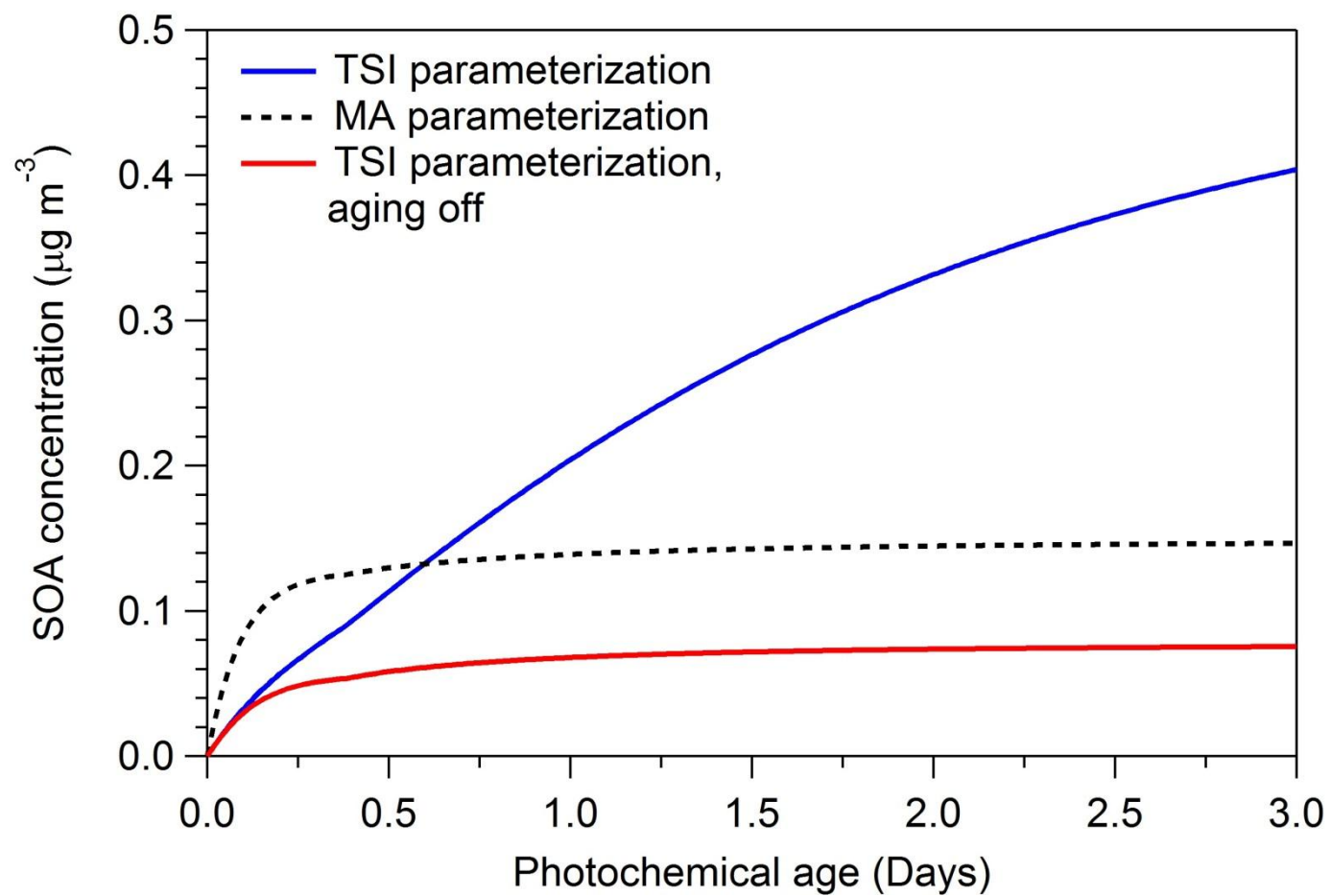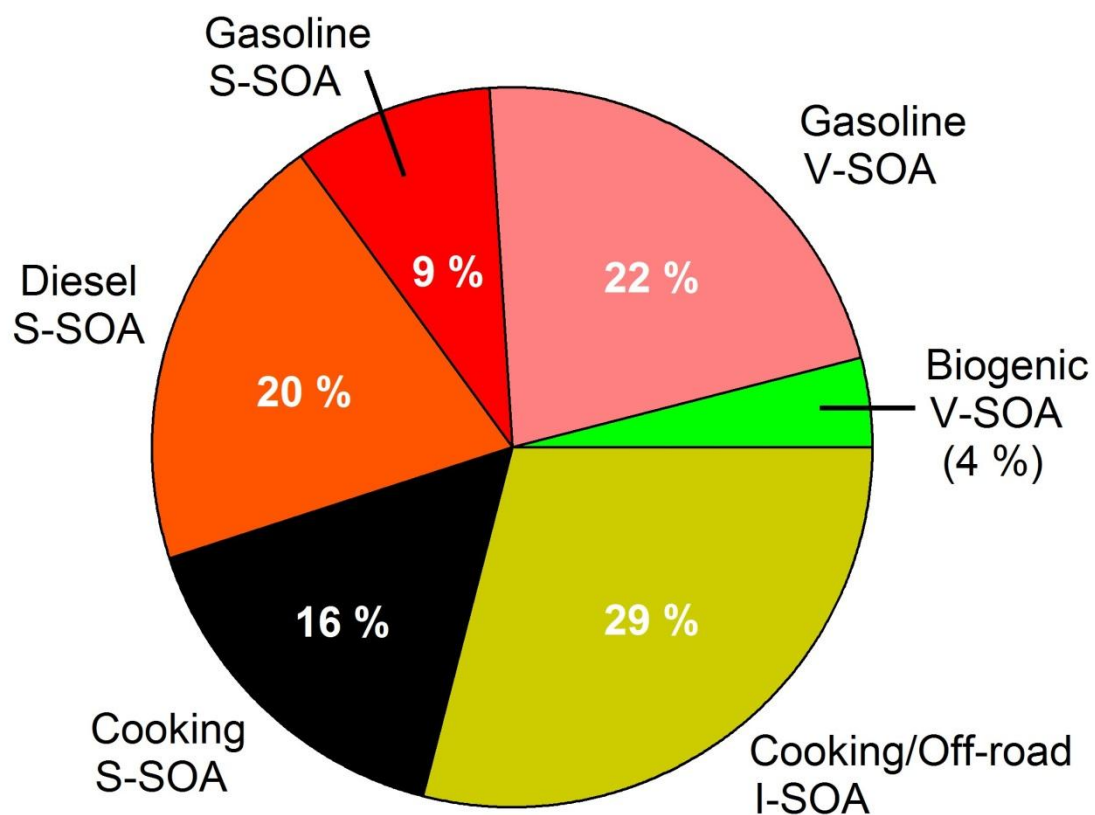92 **Figure S2.** Predicted urban SOA mass from the olefin VOCs (Ole1) for different SOA formation parameterizations.
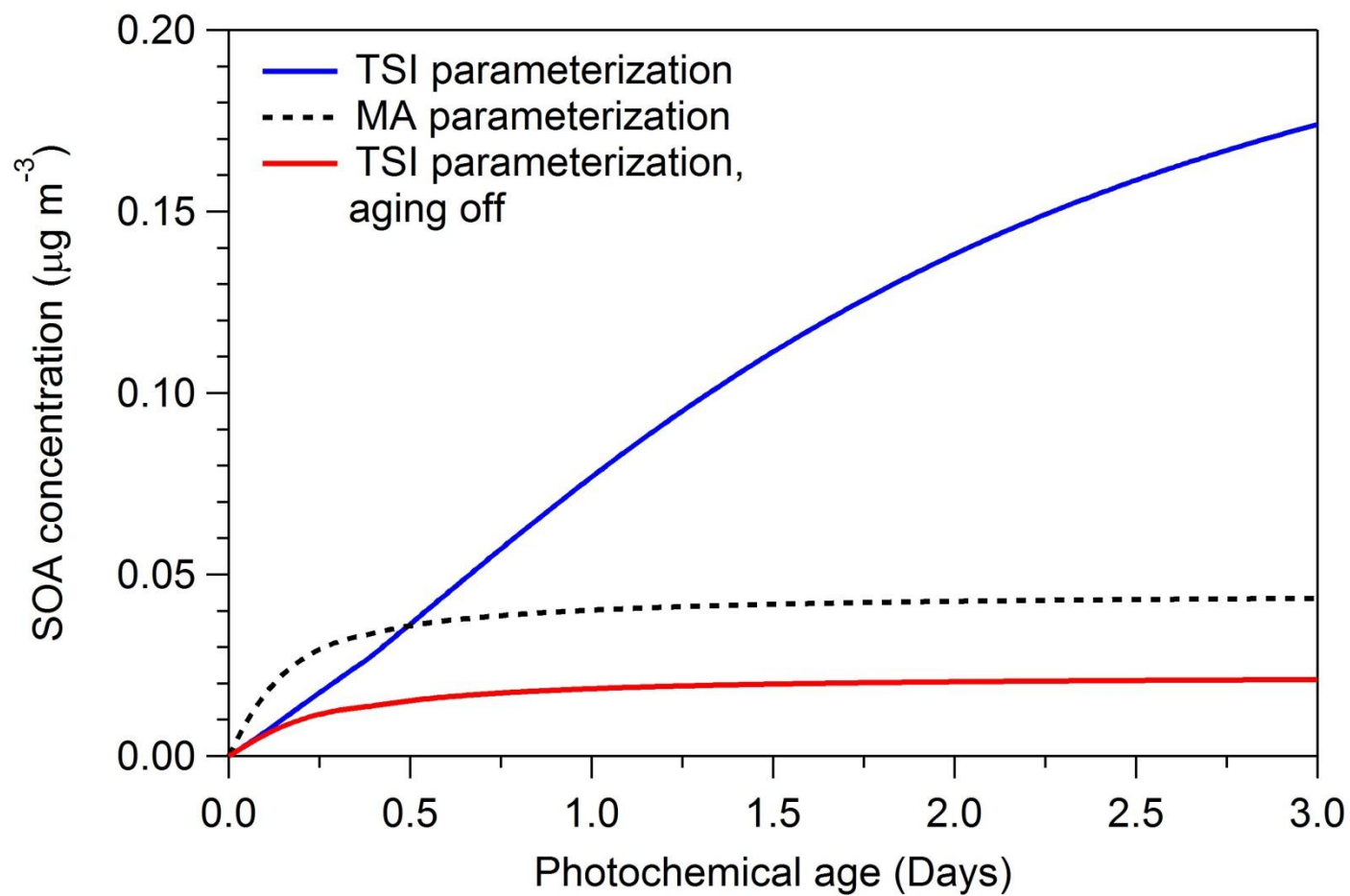
93

94 **Figure S3** Predicted urban SOA mass from the olefin VOCs (Ole2) for different SOA formation parameterizations.
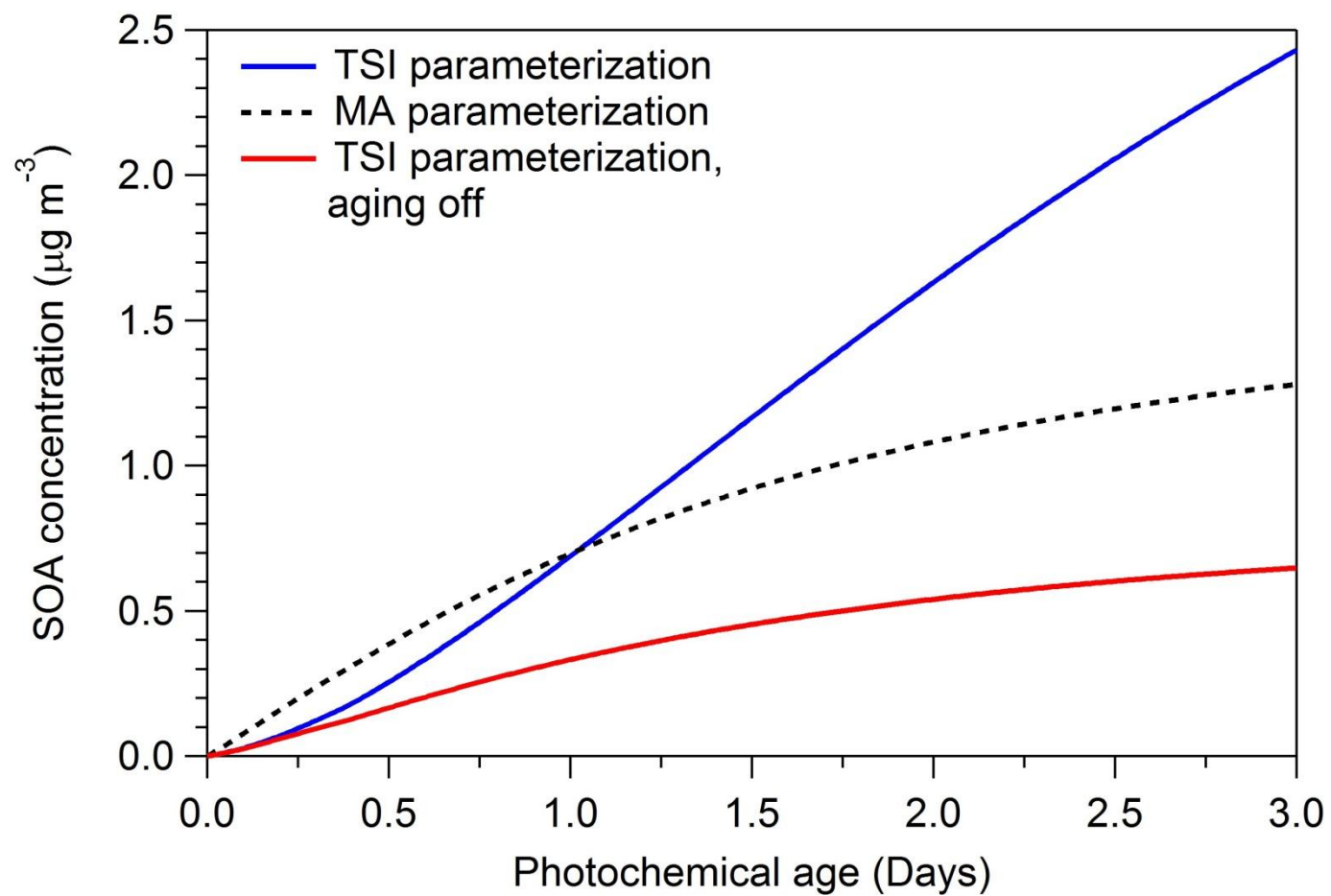
95

96 **Figure S4.** Predicted urban SOA mass from the aromatic VOCs (Aro1) for different SOA formation parameterizations.
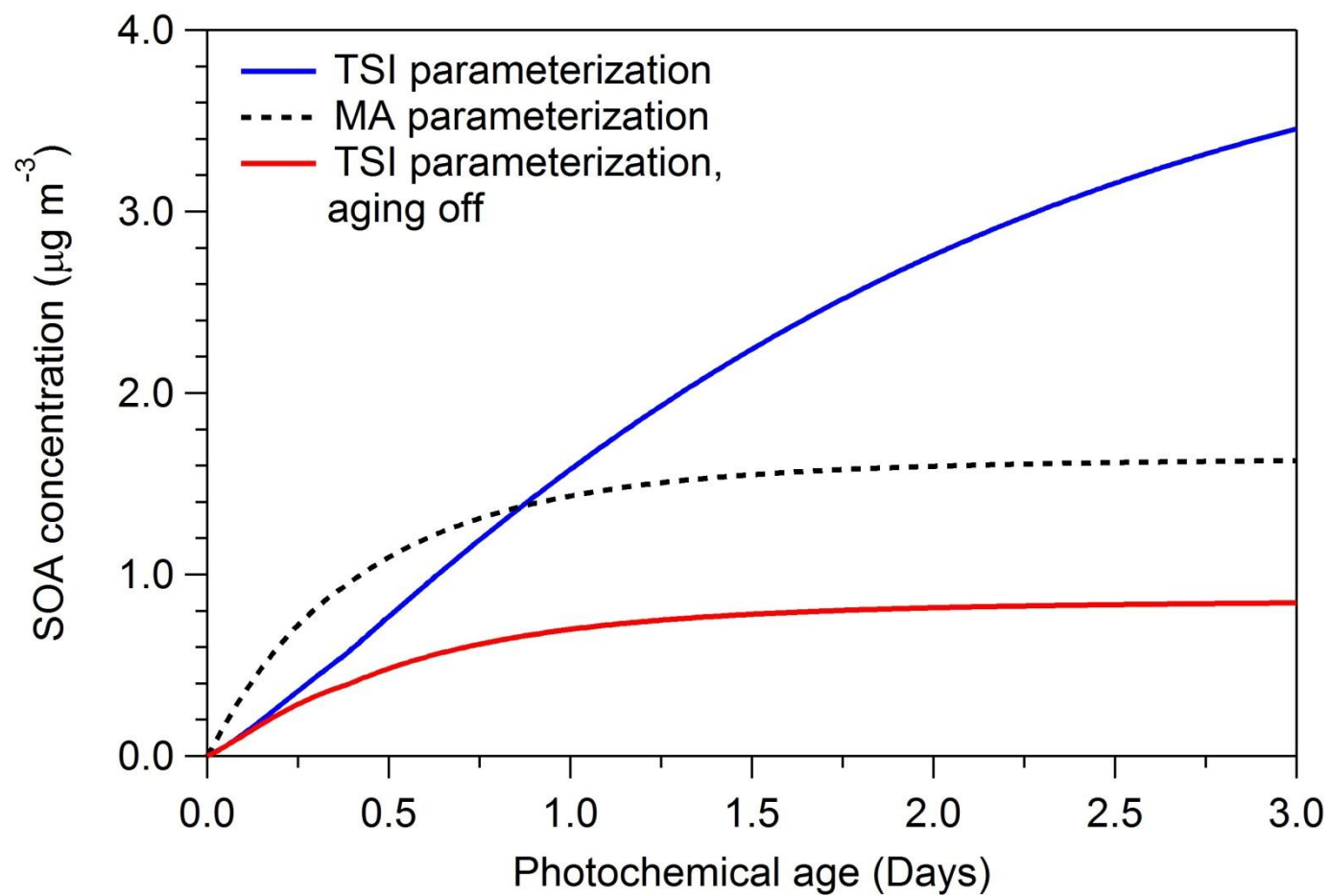
97

98   **Figure S5.** Predicted urban SOA mass from the aromatic VOCs (Aro2) for different SOA formation parameterizations.
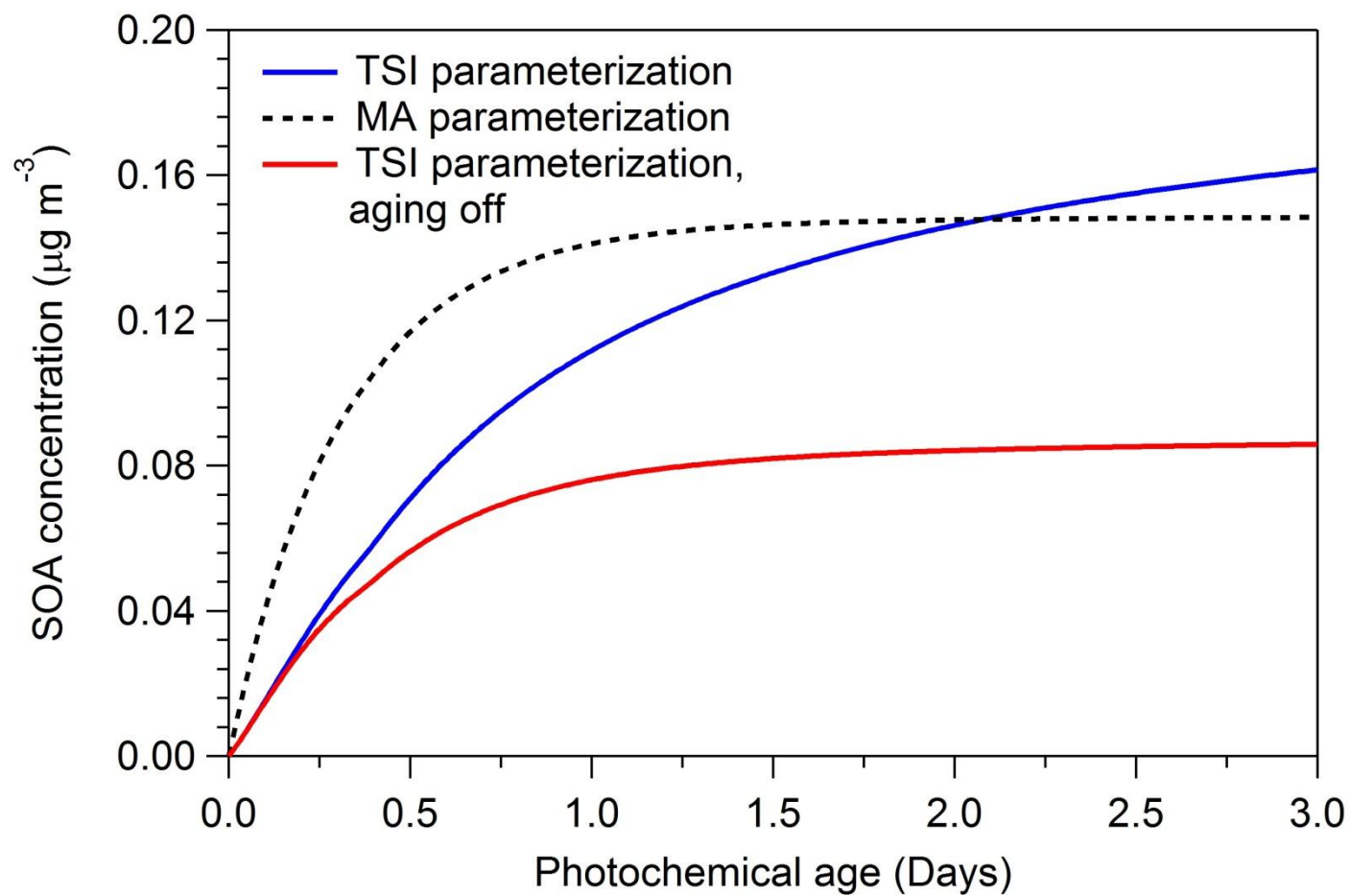
99

100 **Figure S6.** Predicted urban SOA mass from isoprene (Isop) for different SOA formation parameterizations.

101

102   **Figure S7.** Predicted urban SOA mass from terpenes (Terp) for different SOA formation parameterizations.
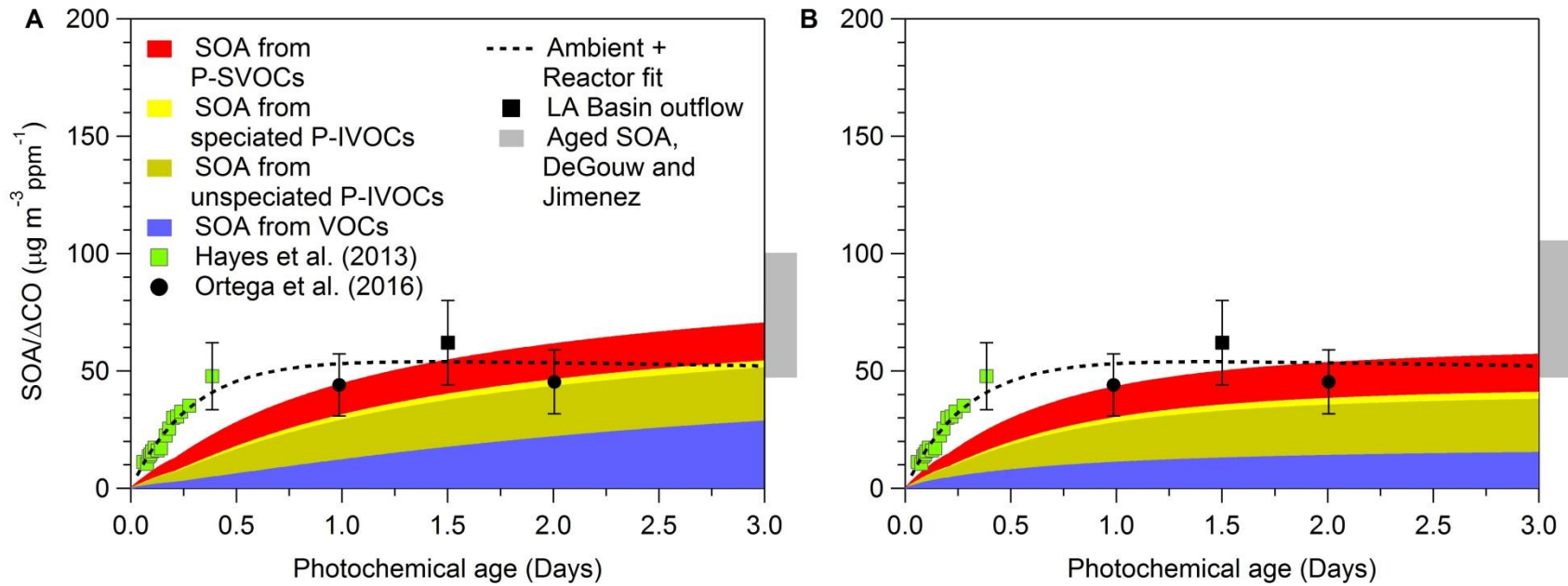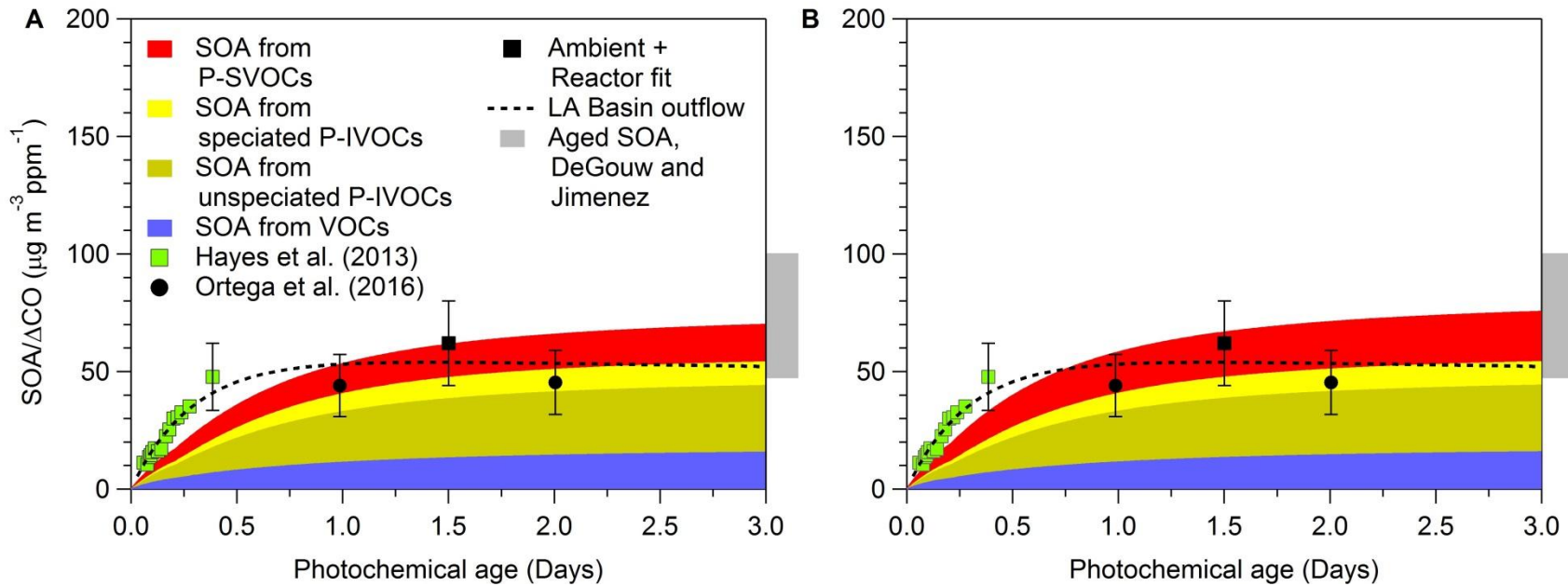
Figure S8. Predicted urban SOA mass by the A) WOR + ZHAO + TSI and B) WOR + ZHAO + MA cases when using the meat cooking volatility distribution reported by Woody et al. (2016).
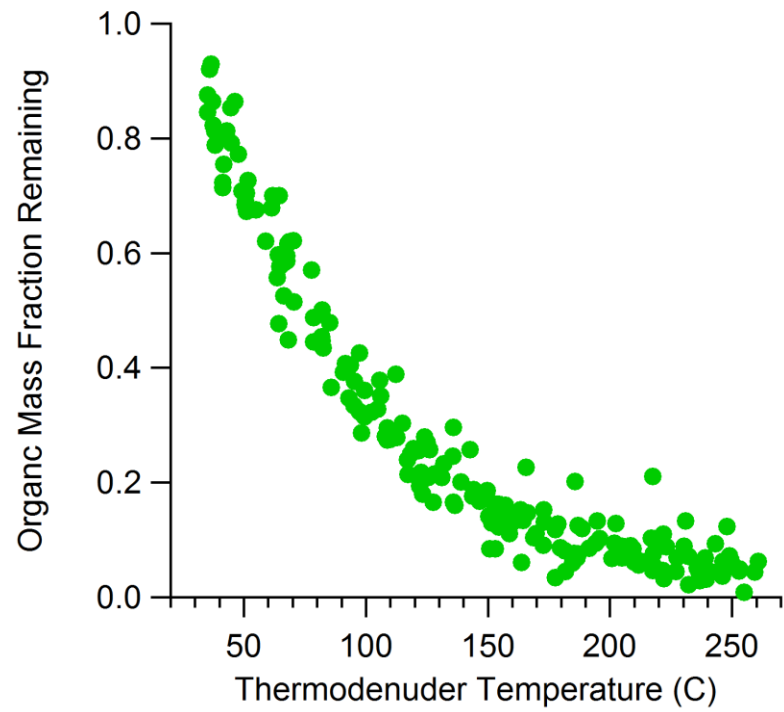
Figure S9. Estimated fractional contributions to urban SOA mass concentration using the WOR + ZHAO + MA case.

106

107

Figure S10. Predicted urban SOA mass for the A) ROB + ZHAO + MA and B) WOR + ZHAO + MA cases when using IVOC initial concentrations determined using photochemical age, the Pasadena IVOC concentrations and the estimated IVOC oxidation rate constants.

112

Figure S11. Organic mass fraction remaining as a function of temperature for Pasadena, California during CalNex 2010. Data correspond to 12:00 – 15:00 local time.